Molecular Characterization of Semi-Fluorinated Copolymers with a Controlled Amount of Long-Chain Branching

Dietmar Auhl, Joachim Kaschta, and Helmut Münstedt*

Institute of Polymer Materials, University Erlangen-Nürnberg, Martensstrasse 7, D-91058 Erlangen, Germany

Harald Kaspar and Klaus Hintzer

Research Department, Werk Gendorf, Dyneon GmbH & Co. KG, D-84504 Burgkirchen, Germany

Received June 28, 2005; Revised Manuscript Received January 31, 2006

ABSTRACT: The molecular structure of various semi-fluorinated polymers derived from tetrafluoroethylene, hexafluoropropylene, and vinylidenefluoride is examined by different characterization methods in dilute solution. The polymer synthesis was tailored to set up samples with a straight linear topography as well as model polymers with a controlled amount of long chain branching. As anticipated from the reaction kinetics of the polymerization process, the absolute molar mass distributions of the linear samples as obtained by size exclusion chromatography coupled with multiangle light scattering are well described by a Schulz−Zimm distribution. With $[\eta] \sim M^{0.73}$ and $\langle s^2\rangle^{1/2} \sim M^{0.53}$ in THF, scaling laws typical of coil dimensions of linear macromolecules in good solvents were observed. In the second set of samples, the presence of long-chain branching (LCB) becomes evident from a reduced radius of gyration in the high molar mass region. Solution viscometry on the polydisperse samples reveals a decreasing contraction factor $g_\eta = [\eta]_{br}/[\eta]_{lin}$ of the intrinsic viscosity (equivalent to g' as introduced by Zimm and Kilb) with increasing amount of branching agent utilized in the polymer synthesis. The branching parameter ϵ determined from g_η together with the contraction factor of the radius of gyration $g_s = \langle s^2\rangle_{br}/\langle s^2\rangle_{lin}$ is found to be increasing from 0.5 for $M < 10^6$ g/mol to about 1.3 at higher molar masses, which is indicative of a topography change from a starlike to a comblike polymer architecture.

Introduction

Fluoropolymers are used in a variety of high performance applications due to their outstanding properties such as high heat and chemical resistance, good weatherability and UV-stability, low surface energies, or good dielectric and optical properties. Fluoropolymers include in particular fluoroelastomers and fluorothermoplasts, which are often copolymers of fluorinated olefins such as tetrafluoroethylene (TFE), chlorotrifluoroethylene (CTFE) and/or vinylidene fluoride (VDF) with one or more comonomers as for example hexafluoropropylene (HFP), perfluorovinyl ethers (PVE), or nonfluorinated olefins such as ethylene (E) and propylene (P).[1−4]

The semicrystalline fluorinated copolymers used in this study are derived from TFE, HFP, and VDF. Melt-processable resins of this ternary monomer combination possess many desirable and beneficial physical properties such as low melting and processing temperature, high resistance to corrosive chemicals, good flexibility, and optical clarity. Besides certain exceptions known from the art,[5] fluoropolymers produced by conventional methods often show a linear chain topography. Applications of the commercially available grades are, for example, items such as tubing, film sheets, and seals.

Some ternary copolymers made of TFE, HFP, and VDF, preferably those ones with a fluorine content of less than 70%, are soluble at room temperature in conventional organic solvents such as tetrahydrofuran, acetone, or methylethyl ketone. Resultantly, these products can be analyzed in dilute solution with respect to the molecular structure by viscometry, size exclusion chromatography (SEC) and light scattering. Nevertheless, solution properties of semi-fluorinated copolymers have been published in only very few articles. Maccone et al.[6] conducted measurements with a light scattering device and size-exclusion chromatography coupled with a viscosity detector on fluoroelastomers polymerized with a iodine chain transfer agent and in the case of one sample in the presence of a diolefin. The authors investigated the molar mass distribution and long-chain branching frequency of the lab scale samples as well as fractionated high molar mass components. The frequency of tri- and tetrafunctional long-chain branches was calculated by an iterative approach and it was found to be in the range of 0.1 to 1 long-chain branch per molecule. The mass-average molar masses of the branched sample fractions were validated by light scattering batch measurements.

The SEC-light scattering combination and solution viscometry, which are used together in the present work, allow the determination of both the radius of gyration and intrinsic viscosity, respectively. Following from that, the contraction factors g_s and g_η can be calculated. A combination of these methods is particularly useful for a thorough investigation of the molecular structure and topography because each method offers specific advantages. Not only is the dimension of the macromolecules well suited for the determination of long-chain branching but also it is a primary parameter needed to understand the physical properties of a polymer, e.g., its rheological behavior.

The positive effects of long-chain branching on the processing behavior of different polymers are known for many years. Rheological properties of the melt measured at a laboratory scale can be correlated with some aspects in the processing behavior. For example, long-chain branching is known to enhance the processing properties in terms of a more homogeneous elongational deformation due to strain hardening. Much academic

* Corresponding author. E-mail: polymer@ww.uni-erlangen.de.

10.1021/ma051391a CCC: $33.50
Published on Web 02/24/2006

Table 1. Molecular Characteristics of the Linear THV Samples as Determined from SEC-MALLS as well as Solution Viscometry and Parameters Used for the Fit of the Schulz−Zimm Distribution

	THV 1	THV 2	THV 3	THV 4	THV 5	THV 6	THV 7
$M_{n,k}$[a] [kg/mol]	104	160.6	468.7	850.9	1052	1532	4000
ξ[a]	1.8	2.0	1.8	1.4	1.3	1.6	1.9
Ψ[a]	69.7	109.9	296.1	581.9	602.3	534.4	350
M_w [kg/mol]	161	242	725	1450	1870	2480	6110
M_w/M_n	1.6	1.5	1.6	1.7	1.6	1.6	1.8
$\langle s^2\rangle_z^{1/2}$ [nm]		22.4	33. 4	53.2	60.6	80.6	121.3
$[\eta]$[b] [mL/g]	33	46	105	171	214	309	432

[a] Parameter as defined in the Zimm−Schulz distribution (eq 6). [b] Determined in MEK at 35 °C using a Cannon−Fenske viscometer.

Table 2. Molecular Characteristics of the Long-Chain Branched THV Samples as Determined from SEC-MALLS and Parameters Used for the Fit of the Molar Mass Distribution

	LCB-THV 1	LCB-THV 2	LCB-THV 3	LCB-THV 4	LCB-THV 5	LCB-THV 6
$M_{n,k}$[a] [kg/mol]	208	220	220	243	149	323
ξ[a]	1.49	1.4	1.46	0.99	1.45	1.26
Ψ_1[a]	28.16	35.40	31.60	31.73	20.40	38.14
M_2[a] [kg/mol]	800	800	750	110	750	950
Ψ_2[a] [10^{-6}]	0.96	2.0	4.0	5.5	2.0	9.0
Ω[a]	0.9	0.9	0.84	0.7	0.8	0.8
M_w [kg/mol]	544.8	684.3	765.2	1030.5	540.5	1316.5
M_z [kg/mol]	2796	3410	2908	2745	2411	3691
M_w/M_n	2.44	2.78	2.87	3.19	3.1	2.89
$\langle s^2\rangle_z^{1/2}$ [nm]	56.8	52.6	47.7	52.0	51.5	60.1

[a] Parameter as defined in the Zimm−Schulz distribution (eq 7).

work regarding the influence of LCB on the flow behavior has been published for bulk resins (Long et al.[7]), especially for polyolefins, e.g. Münstedt and Laun,[8] Gahleitner,[9] Vega et al.,[10] but only a very small amount is known in this field for fluoropolymers. Seeking to close that gap, we conducted a molecular characterization on a set of custom-made fluoropolymer samples prepared in lab scale with independently tailored molecular mass and polymer topography.

Materials and Methods

Samples. The $TFE_{39}/HFP_{11}/VDF_{50}$ terpolymers, referred to as THV terpolymers in the following, were prepared by means of aqueous emulsion polymerization conducted in a 48.5 l pilot plant reactor (Dyneon GmbH & Co. KG) made of stainless steel and equipped with an impeller agitator system. After the oxygen-free reactor was charged with deionized water, emulsifier, buffer, and appropriate chain transfer agent, a composition of gaseous monomers consisting of 44 mol % HFP, 30 mol % VDF, and 26 mol % TFE was precharged to reach an absolute pressure of 15.5 bar. After initiation of the polymerization by a water-soluble initiator, the chemical composition of the copolymer formed during the course of polymerization was controlled. Herein, the reaction pressure and reaction temperature was maintained by feeding 39 mol % TFE, 11 mol % HFP, and 50 mol % VDF into the gas phase using a computer controlled on-line flow metering system.

A first set of THV terpolymers was synthesized at low polymerization temperatures to avoid transfer reactions to the hydrogen containing polymer backbone. Accordingly, the samples obtained are expected to show a straight linear chain topology. As disclosed for instance by Kaspar et al.,[11] the molecular weight was controlled by the amount of an appropriate chain transfer agent. The characteristic data of the thus-obtained polymer samples are summarized in Table 1. A second set of copolymer resins with the same chemical composition was prepared in the presence of an additional modifier, which induces some degree of transfer reactions to the polymer backbone during the polymer synthesis. The technique applied enables one to keep control over the long-chain branching formation during the entire polymerization process. For the samples listed in Table 2, the amount of LCB as well as the molar mass have both been tailored.

Experimental Data. SEC experiments were carried out at 25 °C with analytical grade tetrahydrofuran (THF, Merck KGaA) using a Knauer HPLC pump and a Bischoff RI 8100 differential refractive index detector (DRI). The column set consisted of four UltraStyragel columns (Waters Corp., 10^3-10^6 Å). A constant flow rate of 1 mL/min was used. The SEC was coupled with a DAWN EOS multiangle laser light scattering detector (MALLS) of Wyatt Technology Corp., which has 18 measuring angles between 17° and 155°. The data acquisition and analysis was carried out using the software WinGPC V.6.0 (PSS, Polymer Standards Service GmbH) as well as ASTRA v4.73.04 (Wyatt Technology Corp.). The software used for calculation of the number of LCB was CORONA v1.40 (Wyatt Technology Corp.). Solutions with a concentration of 3 g/L have been prepared by dilution and filtered with a 0.2 μm filter in order to remove dust and aggregates. Monodisperse polystyrene (PS) standards with polydispersities M_w/M_n of about 1.03 and mass-average molar masses between 5.80×10^2 g/mol and 7.50×10^6 g/mol (Polymer Laboratories GmbH) were used in order to determine the calibration curve $M(V_{el})$ for the experimental set up. Batch measurements with the MALLS detector were conducted on polydisperse solutions of linear THV 4 and long-chain branched LCB-THV 3 in THF at 25 °C. Solutions of concentrations between 1.5 and 6 g/L in THF were prepared in glass flasks and injected through a 0.2 μm filter directly into the flow cell of the MALLS detector. The software used for calculation of the Zimm diagrams was ASTRA V4.73.04 (Wyatt Technology Corp.). The intrinsic viscosities $[\eta]$ were measured in methylethyl ketone (MEK) at 35 °C using a Cannon-Fenske viscometer (Schott AG) for polydisperse fractions. A concentration of 2 g/L was analyzed and the Hagenbach−Couette correction, e.g., the kinetic energy correction of the flow time in the capillary, was applied.

Results and Discussion

Molar Mass Distribution from SEC-MALLS Measurements. Long-chain branched molecules possess a smaller hydrodynamic radius compared to linear molecules of the same molar mass.[12,13] As a result, the conventional SEC using linear polymer standards for calibration is incapable to determine the absolute molar mass distribution of branched polymer structures. Moreover, the parameters α and K of the well-known Kuhn−Mark−Houwink−Sakurada (KMHS) equation $[\eta] = KM^{\alpha}$ are often not known for copolymers. For branched copolymers, however, these complications can easily be overcome by a coupling of a conventional SEC with a MALLS device. This coupling enables one to determine the absolute molar mass M_{LS} of every slice of the chromatogram directly at each elution

volume V_e. The molar mass distributions of all samples are determined by the measured concentration signal $c(V_e)$ and the calibration curve $M(V_e)$ as described for example by Shortt:[14]

$$w(M) = -\frac{\log e}{M(V_e)} \frac{c(V_e)}{\mathrm{d}M(V_e)/\mathrm{d}V_e} \quad (1)$$

The concentration $c(V_e)$ is taken from the refractive index signal of the DRI detector and the absolute molar masses $M(V_e)$ were measured by light scattering using the well-known light scattering equation:[15,16]

$$\frac{Kc(V_e)}{\Delta R(\Theta,c)} = \frac{1}{M_w(V_e)P(\Theta)} + 2A_2c(V_e) \quad (2)$$

Herein, K is the optical constant of the light scattering device, which is equal to $4\pi^2n^2(\mathrm{d}n/\mathrm{d}c)^2/\lambda_0^4N_a$, $\Delta R(\Theta, c)$ is the excess Rayleigh ratio at the angle Θ of scattered light relative to the incident beam, $P(\Theta)$ is the form factor, n is the refractive index of the solvent, N_a is Avogadro's number, and λ_0 is the in vacuo wavelength of the incident light.

A crucial input parameter for the determination of the absolute molar mass distributions is the refractive index increment dn/dc. This specific value describing the change in refractive index n of a solution with concentration c at a fixed wavelength and a fixed temperature is needed twice; first, for calculating the concentration $c(V_e)$ from the signal of the DRI detector, and second, for the absolute molar masses $M(V_e)$ from light scattering. The absolute molar mass is linearly dependent on the value of dn/dc if measured by SEC-MALLS using a DRI detector as a concentration detector. As the molar mass is even squared proportional in the case of light scattering batch measurements—an error in dn/dc will necessarily result in a relatively large error in molar masses.

The dn/dc value of a polymeric solution can be estimated from the refractive indices of both components (n of the polymer and n_0 of the solvent) according to the Dale−Gladstone[17] equation:

$$(\mathrm{d}n/\mathrm{d}c)_{T,\lambda_0} = \frac{\mathrm{d}n}{\mathrm{d}c}\Big|_{T,\lambda_0,c=0} \approx \frac{n-n_0}{\rho_0}\Big|_{T,\lambda_0} \quad (3)$$

Accordingly, a dn/dc of around −0.05 mL/g is estimated for the polymeric solution using the refractive index for the THV terpolymer investigated ($n = 1.36$) and the value for the pure solvent ($n_0 = 1.41$ for THF with $\rho_0 = 0.9$ g/mL at 25 °C). The low scattering intensity of the THV terpolymer in THF cannot easily be improved by the selection of another possible solvent such as methylethyl ketone ($n_0 = 1.38$) or acetone ($n_0 = 1.36$). In these two cases, isorefractive solutions will be obtained that cannot be analyzed by a DRI detector (dn/dc becomes close to zero).

The molar mass dependence of dn/dc was shown by Hadjichristidis and Fetters,[18] for example, both for linear and branched polystyrenes and polyisoprenes with different number-average molar masses dissolved in toluene and cyclohexane, respectively. For the samples of sufficiently high molar mass the value of dn/dc is nearly independent of molar mass since the so-called end group effect can be neglected. The authors have also shown that dn/dc is not influenced by the branching ratio.

In principle, dn/dc can be determined on-line by chromatographic measurements if the concentration of the sample solution, the injected volume, the calibration constant of the DRI detector, and the flow rate are known exactly and if a total elution of the polymer from the columns is assumed. The method is not very accurate and not favorable because of the experimental difficulties and multiple sources of errors for the refractive index increment. Therefore, dn/dc is determined directly by measuring the refractive index of solutions with different concentrations. The dn/dc values of the linear sample THV 3 and a commercial PS (Polystyrol 158K, BASF AG) were determined at 25 °C using a DAWN DSP−F detector (Wyatt Technology Corp.) at two different wavelengths $\lambda_0 = 488$ nm and $\lambda_0 = 633$ nm and the DRI detector at $\lambda_0 = 950$ nm. At least three different concentrations between 1 and 5 g/L were measured. The dependence of dn/dc on the wavelength λ_0, the so-called dispersion, is plotted in Figure 1. Some confidence is gained regarding the reliability of the experiments and the wavelength dependence from the comparison of the measured values with literature data published for PS in THF at a slightly higher temperature of 30 °C.[19−21]

The value of dn/dc is a function of temperature and of the wavelength of the light source used. For the determination of the accurate dn/dc value the wavelength dependence was incorporated by interpolating to $\lambda_0 = 690$ nm, which is the wavelength of the laser used in the MALLS detector, using a quadratic relation. This yields a value of −0.037 mL/g for the THV samples. This dn/dc is reasonable if compared to the value

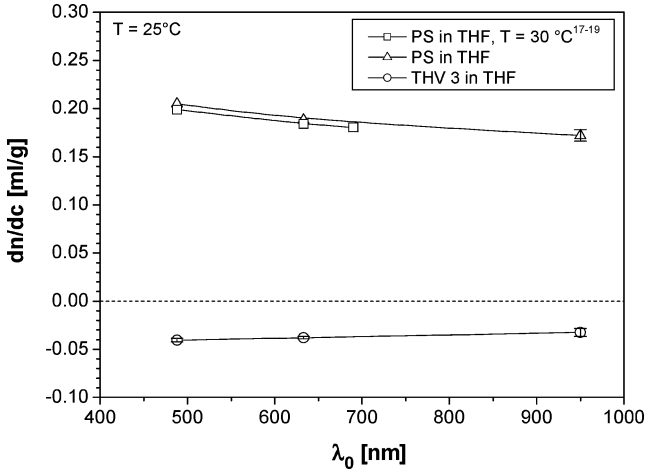

Figure 1. Refractive index increment dn/dc as a function of laser wavelength λ_0 for the linear fluoropolymer THV 3 and polystyrene in THF at $T = 25$ °C.

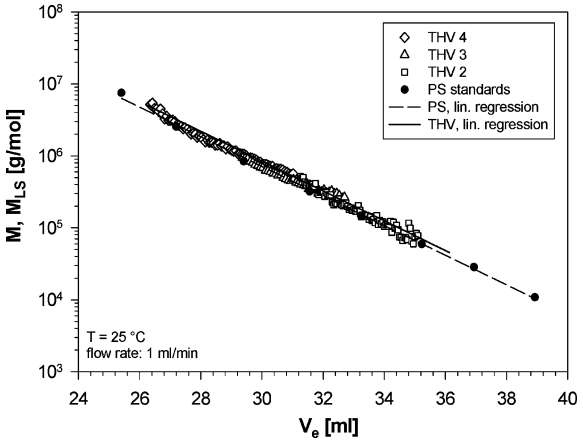

Figure 2. Molar masses M and M_{LS} as a function of elution volume V_e as determined by SEC for PS standards and SEC-MALLS for linear THV samples.

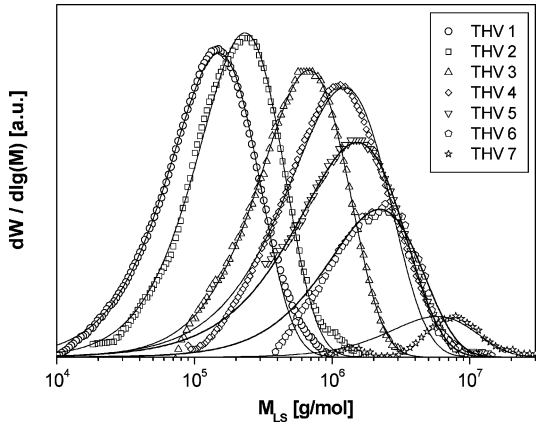

Figure 3. Molar mass distributions for linear THV samples as determined from SEC-MALLS. The full lines are fits using eq 6.

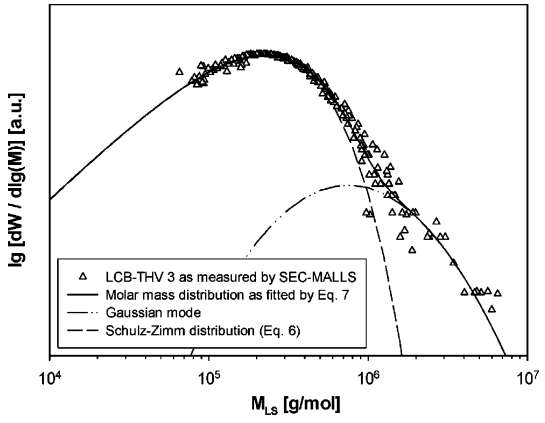

Figure 4. Molar mass distribution of LCB-THV 3 as measured by SEC-MALLS and fitted by eq 7. The ordinate is plotted in a logarithmic scale in order to show the tailing at high molar masses more clearly.

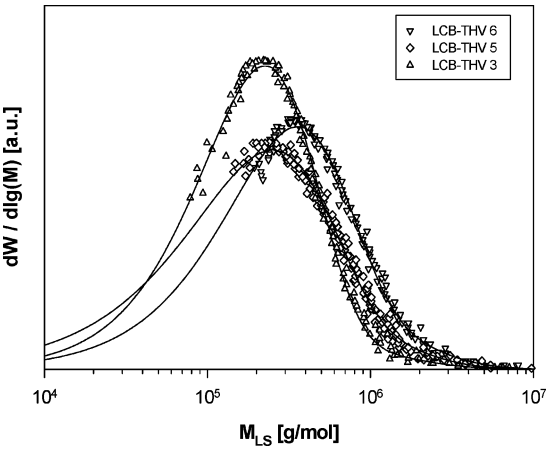

Figure 5. Molar mass distributions of the long-chain branched fluoropolymers with equal amount of branching agent as measured by SEC-MALLS. The full lines are fitted using eq 7 with the additional Gaussian mode.

calculated using eq 3. The d*n*/d*c* determined by the on-line technique as described above was found to be around -0.03 ± 0.01 mL/g but shows strong scattering. Maccone et al.[6] report values ranging from -0.024 mL/g to -0.029 mL/g for semi-fluorinated polymers of a different composition ($TFE_{10}/HFP_{18}/VDF_{72}$ terpolymers) in THF at 30 °C and 630 nm. The slightly smaller absolute value for d*n*/d*c* can be understood from the lower fluorine content of 66% (vs 70% in our case).

The calibration curve $M(V_e)$ of the experimental set up was determined using the PS standards and from that the following relation between the molar mass M and the elution volume V_e was found by linear regression (cf. Figure 2).

$$\log M_{PS}(V_e)[\text{THF},25°\text{C}] = 12.309 - 0.215V_e \qquad (4)$$

For linear THV samples, the following relation was determined by linear regression for the absolute molar mass M_{LS} in g/mol as a function of the elution volume V_e in milliliters over a broad range of molar masses between about 10^4 and 10^7 g/mol:

$$\log M_{THV}(V_e)[\text{THF},25°\text{C}] = 11.897 - 0.200V_e \qquad (5)$$

Using the concentration c and the absolute molar mass M_{LS} measured by SEC-MALLS as a function of elution volume V_e, the molar mass distributions of the linear fluoro-copolymers can be determined using eq 1. The results of the linear THV samples are plotted in Figure 3. The molar mass distributions measured by SEC-MALLS are fitted by a Schulz−Zimm distribution function, which is highly probable for the reaction mechanism and the polymerization conditions used:[22]

$$w(M) = \Psi\frac{\beta^{\xi} + 1M^{\xi}\exp(-\beta M)}{\Gamma[\xi + 1]} \qquad (6)$$

where ξ, is the degree of coupling, which determines the broadness of the molar mass distribution and $\Gamma[\xi+1]$ is the Γ function, which was approximated for the calculation by a seventh-order polynomial fit. The parameter Ψ is used as a scaling factor. Furthermore, β is equal to the ratio $\xi/M_{n,k}$ where $M_{n,k}$ is the number-average molar mass of the kinetic chain. Thus, only the two independent parameters β and ξ have to be adjusted by the fitting algorithm.

The Schulz−Zimm distribution functions fitted to the experimental data of the different linear THV samples are indicated by the full lines in Figure 3. By using this model the experimental data can be extrapolated at the boundaries and the statistical scattering was reduced. A very good agreement is found for the whole molar mass distribution in the case of the samples with low and medium M_w values. Some deviations from SEC-MALLS data are found especially in the low molar mass range of the high molar mass samples, which can be ascribed to the difficulties in measuring the low concentration signal $c(V_e)$ for these samples. The parameters determined for the adjustment are provided in Table 2. They show a very reasonable agreement with model predictions as the number-average molar mass of the kinetic chain $M_{n,k}$ increases while the degree of coupling is very similar and in the range 1.4−1.9. This is consistent with the reaction kinetic model for this type of polymerization process, which predicts values between 1.5 and 2.

The molar mass averages M_n, M_w, and M_z were calculated on a linear scale from the fitted Schulz−Zimm distribution function $w(M)$ in equidistant slices of 1000 g/mol. The average molar mass values of the different linear samples cover a wide range as it was intended in the polymerization process (cf. Table 1). From the polydispersity ratio M_w/M_n it can be concluded that the linear THV samples have got a quite narrow molar mass distribution. For the samples with higher M_w the polydispersity increases only slightly.

In contrast to the linear samples, the measured data of the long-chain branched samples cannot be reasonably described by using eq 6, solely. But for the calculation of correct average

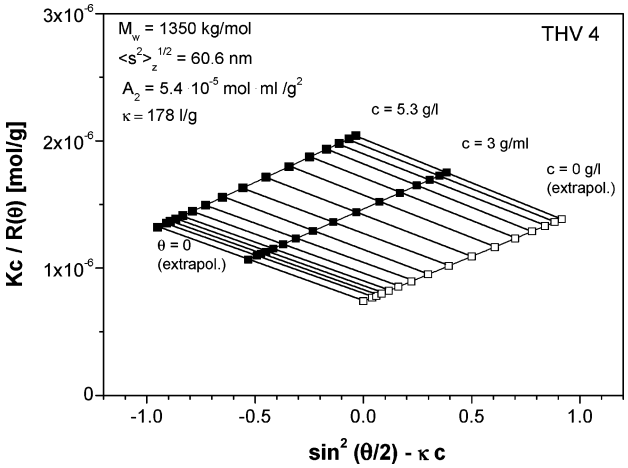

Figure 6. Zimm plot of THV 4 as measured by MALLS in THF at 25 °C.

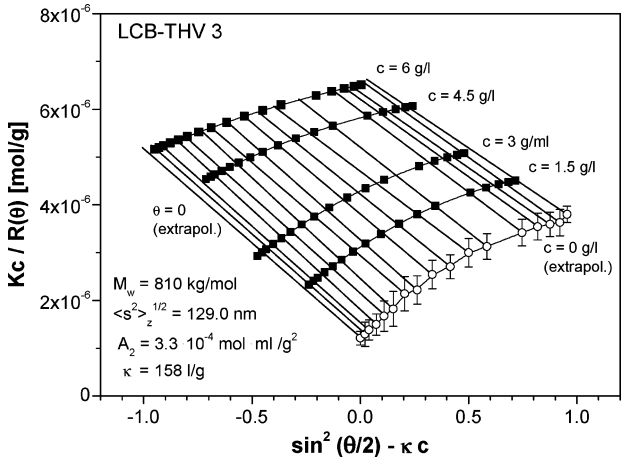

Figure 7. Zimm plot of LCB-THV 3 as measured by MALLS in THF at 25 °C.

molar masses (cf. Figure 4), the consideration of the tailing at high molecular masses is mandatory. For this reason, the high molecular weight tailing was empirically modeled by a distribution function of a logarithmic Gaussian type added to the Schulz−Zimm distribution function:

$$w(M) = \Psi_1 \frac{\beta^{\xi} + 1 M^{\xi} \exp(-\beta M)}{\Gamma[\xi + 1]} + \Psi_2 \exp\left[-0.5\left(\frac{\ln(M/M_2)}{\Omega}\right)^2\right] \quad (7)$$

The parameters used for the Gaussian term are M_2, Ψ_2, and, Ω, which correspond to the position, height, and, width of the high molar mass tailing.

The molar mass distributions of the long-chain branched samples as measured by SEC-MALLS are shown in Figure 5 for the samples with equal amount of branching agent. In this set, the samples of high molecular weight show slightly higher polydispersities due to a more pronounced tailing at high molar masses. The samples LCB-THV 1 to LCB-THV 4 on the other hand, show only slight differences of the polydispersity and mass-average molar mass although they are polymerized under the presence of different amounts of branching agent.

Light Scattering Batch Measurements. Batch measurements can be conducted with a small amount of material and without any prior fractionation by SEC columns. In this mode the mass-average molar mass M_w and the *z*-average root-mean-square radius of gyration $\langle s^2\rangle_z^{1/2}$ as well as the second virial coefficient A_2 of the total sample can be determined from Zimm diagrams. Since the result of the *off-line* determination is affected by residual dust or aggregates, the accuracy of the so-obtained radius of gyration and molar mass averages is not necessarily higher compared to those calculated for the fractionated samples. Nevertheless, these batch measurements are very useful to verify the analysis of the fractionated samples since absorption of high molar mass components or shear degradation of molecules may have been occurred in the SEC columns.

In Figures 6 and 7, the Zimm diagrams are plotted for the linear sample THV 4 and the long-chain branched sample LCB-THV 3, respectively. In this diagram, the intercept of the line at $\theta = 0$ at the ordinate yields the reciprocal mass-average molar mass M_w and the slope yields the root-mean square radius of gyration.[15] For the linear sample THV 4, M_w was found to be 1.35×10^6 g/mol in comparison to a value of 1.45×10^6 g/mol as determined from SEC-MALLS. For LCB-THV 3, M_w was found to be 8.10×10^5 g/mol compared to a value of 7.65×10^5 g/mol. From that it can be seen that the mass-average molar masses M_w, which have been determined by the two different techniques of chromatographic and of light scattering batch measurements, show reasonably good agreement. The second virial coefficient A_2 was found to be in the order of 10^{-5} and positive. Thus, it is verified that the value is small enough to exclude the second term from the concentration dependence of the light scattering equation (eq 2). The positive value indicates that THF is a good solvent for the THV terpolymers and further, the so-called Θ temperature (where $A_2 = 0$) is lower than 25 °C. However, as can be seen for the Zimm diagram shown in Figure 7, a linear approximation for the angular dependence of the root-mean square radius of gyration does not longer hold. As will thoroughly be analyzed in a forthcoming publication, this deviation is most probably affected by the form factor of the long-chain branched populations being present in the sample LCB-THV 3.

Radius of Gyration from SEC-MALLS. Because SEC-MALLS provides both the molar mass $M_{LS,i}$ and the *z*-average root-mean-square radius of gyration $\langle s^2\rangle_{z,i}^{1/2}$ for each fraction *i* of the sample, it is possible to evaluate the dependence of $\langle s^2\rangle^{1/2}$ as a function of molar mass M_{LS} under the solvation conditions used. The molar mass dependence is a power law $\langle s^2\rangle^{1/2} = KM_{LS}^{\alpha}$. As long-chain branched molecules have smaller radii of gyration at the same molar mass compared to linear molecules, a deviation from the power law toward smaller radii of gyration is a clear indication for the presence of long-chain branching. The molar mass dependence of the radius of gyration for monodisperse fractions of different linear THV samples was determined in the range between about 2×10^5 and 10^7 g/mol (Figure 8). The determination of the radius of gyration is limited for low molar masses. For molecules with a radius of gyration smaller than 20 nm the scattering of the laser beam becomes more and more isotropic and the angular dependence, which is used for calculating the radius of gyration, disappears.

By combining the data of the linear samples with different mass-average molar masses, it was possible to confidently analyze the dependence of the radius of gyration on molar mass in a relatively broad range of molar masses although the indiviual sample has a narrow molar mass distribution. The data sets used have been restricted to the range where reliable results have been obtained for $\langle s^2\rangle^{1/2}$ and M_{LS}. Additionally, the radius of gyration $\langle s^2\rangle_z^{1/2}$ was plotted for THV 2 to THV 7 at their *z*-average molar masses M_z, which were calculated from the Schulz−Zimm distribution. Linear regression yields the fol-

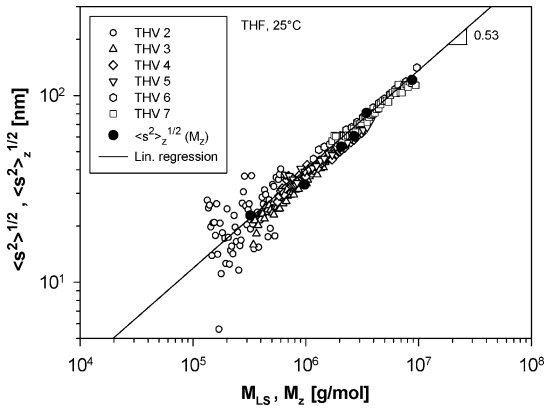

Figure 8. Root-mean-square radius of gyration of $\langle s^2\rangle^{1/2}$ as a function of molar mass M_{LS} for linear THV as measured by SEC-MALLS in THF at 25 °C.

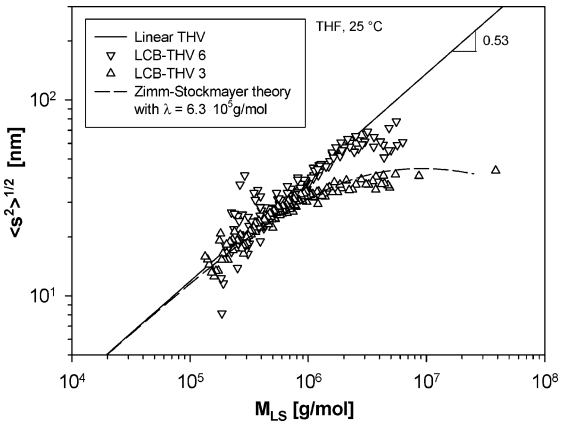

Figure 9. Root-mean-square radius of gyration $\langle s^2\rangle^{1/2}$ as a function of molar mass M_{LS} for different LCB-THV samples as measured by SEC-MALLS in THF at 25 °C. The dashed line corresponds to eq 9.

lowing power law $\langle s^2\rangle^{1/2} = 2.66 \times 10^{-2} M_{LS}^{0.53}$ for $\langle s^2\rangle^{1/2}$ in units of nanometers and M_{LS} in grams per mole, respectively. The value of 0.53 for the slope of the molar mass dependence of the radius of gyration has got an experimental error margin of about ±0.03 due to the inherent scattering of SEC-MALLS data. Some data show significant scattering because of the relatively low molar masses and small refractive index increment of the samples, which is a widely known and limiting experimental problem for a number of materials.[6,23] However, this value for the slope α is reasonable for linear polymers in good solvents. It is only slightly smaller than the theoretical value of 0.588 predicted for good solvents by the renormalization theory. Furthermore, the value is found to be in good agreement with the value calculated from the slope α of the molar mass dependence of the intrinsic viscosity using the Flory−Fox equation.[24,25]

The molar mass dependence of the radius of gyration for linear THV samples can now be used for the branching analysis of the long-chain branched THV samples. In Figure 9, the radius of gyration as a function of molar mass is shown for two long-chain branched samples with different mass-average molar masses. At high molar masses, the radius of gyration $\langle s^2\rangle^{1/2}$ deviates for both samples toward smaller values but is more pronounced for LCB-THV 3. The deviation increases with molar mass and reaches a plateau. This behavior clearly indicates long-chain branching. A similar dependence is found for statistically branched polymers with a branching content increasing with molar mass, e.g., the work of Jackson et al.[26] and Gabriel and Münstedt.[27] The shape of the curve can be explained by the polymerization process as the number of the long-chain branches and therefore the contraction of the molecules becomes larger at higher molar masses.

More detailed information on the long-chain branching structure can be extracted from the light scattering data by comparing the mean square radius of gyration $\langle s^2\rangle$ of the branched molecules and linear counterparts of the same molar mass. The ratio of the mean square radius of gyration of branched polymer $\langle s^2\rangle_{br}$ to that of a linear polymer $\langle s^2\rangle_{lin}$ is represented by the contraction factor or so-called branching index g_s.[28]

$$g_s = \frac{\langle s^2\rangle_{br}}{\langle s^2\rangle_{lin}} \tag{8}$$

The contraction factor g_s can be used to calculate the number of long-chain branches for each molar mass if one assumes Θ conditions under which the dimension of the macromolecules is in the unperturbed state. For the branched fluoropolymers of this study, a trifunctional and randomly branched architecture is anticipated from the statistics of the polymerization process. According to the theory of Zimm and Stockmayer[28] the parameter g_s can be related to long-chain branching in the case of polydisperse samples with a weight-average number of branching points per molecule n_w

$$g_s(n_w) \approx \frac{6}{n_w}\left[0.5\left\{\left(\frac{2+n_w}{n_w}\right)^{0.5} \ln\left(\frac{(2+n_w)^{0.5}+n_w^{0.5}}{(2+n_w)^{0.5}-n_w^{0.5}}\right)^{0.5}\right\} - 1\right] \tag{9}$$

with $n_w = M_w/\lambda$ and λ the average molar mass of a trifunctional monomeric subunit. Herein, it is assumed that the long-chain branching and molar mass of each slice of the SEC-MALLS chromatogram are polydisperse rather than monodisperse because linear and differently branched molecules could have equal hydrodynamic volumes and could elute at the same time. That means, the average number and average length of the branches could be polydisperse in every slice. The molar masses of these species are different, too, so that a mass-average molar mass M_w is detected.

The experimental data set of LCB-THV 3, which has the smallest scatter of the data, can be described by using eq 9 and a molar mass of a branched subunit of $\lambda = 6.3 \times 10^5$ g/mol. The radius of gyration as calculated from the resulting contraction factor g_s is plotted in Figure 9 vs the molar mass M_{LS}. In the low molecular mass region no deviation of the radius of gyration was found for the long-chain branched samples in comparison to the linear samples and g_s is equal to 1. In particular, in the high molecular mass range, a deviation toward higher molar masses is obvious. The value assumed for λ is in good agreement with these observations as relatively long branches lead to a significant reduction of the radius of gyration only at very high molar masses.

Intrinsic Viscosities. As the SEC-MALLS was calibrated using monodisperse polystyrene standards in THF at 25 °C, the intrinsic viscosity $[\eta]_i$ of each elution volume of the chromatogram can be determined from the absolute molar masses $M_{LS,i}$ and the elution volume $V_{e,i}$ for the linear THV samples according to the principle of SEC.[12] The intrinsic viscosity $[\eta]_i$ is calculated for the linear THV terpolymers by the following equation:

$$[\eta]_{THV,i} = [\eta]_{PS,i}\frac{M_{PS,i}}{M_{LS,THV,i}} \tag{10}$$

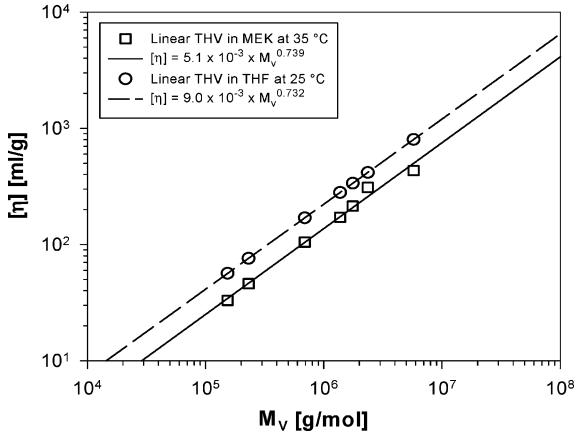

Figure 10. Intrinsic viscosity $[\eta]$ as a function of M_v determined from GPC-MALLS in THF at 25 °C and from off-line viscometry in MEK at 35 °C.

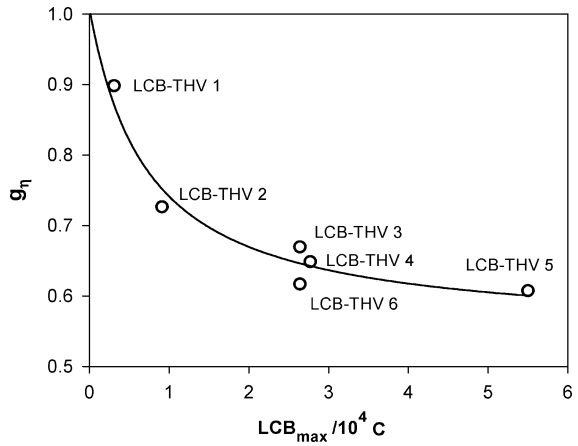

Figure 11. Contraction factor g_η as a function of the maximum number of long-chain branches per 10^4 carbon atoms LCB_{max} for polydisperse LCB-THV samples as measured by solution viscometry in MEK at 35 °C.

For polystyrene dissolved in THF at 25 °C the values for α and K of the KMHS equation are reported in the literature[19] and the following relation is valid:

$$[\eta]_{PS} = 1.60 \times 10^{-2} M^{0.706} \tag{11}$$

In this equation as well as in the following ones, the same units have been used and $[\eta]$ is given in liters per gram and M_v in grams per mole, respectively. The intrinsic viscosities $[\eta]$ of the polydisperse samples were determined at the corresponding viscosity-average molar masses M_v of each sample, which was calculated with $\alpha \approx 0.73$ according to the following relation:[22]

$$M_v \approx (1 - \alpha)(M_n/2) + (1 + \alpha)(M_w/2) \tag{12}$$

For the linear THV samples, the relation of the intrinsic viscosity $[\eta]$ vs the molar mass M_v can be determined from a linear regression of the data measured by SEC-MALLS in THF in Figure 10. Thereby the following relation and thus the parameters α and K are obtained.

$$[\eta]_{THV}\,(\text{THF},25°\text{C}) = 9.0 \times 10^{-3} M_v^{0.732} \tag{13}$$

Furthermore, the intrinsic viscosity $[\eta]$ was measured off-line in MEK at 35 °C by capillary viscometry for polydisperse solutions of the linear and long-chain branched samples. The intrinsic viscosity was obtained from the reduced viscosity η_{red} using the Huggins equation and a Huggins constant of $k_H = 0.34$:

$$[\eta]_{red} = \frac{1}{c}(\eta_{rel} - 1) = [\eta] + k_H c[\eta]^2 \tag{14}$$

with η_{rel} being the relative viscosity.[22] The values for $[\eta]$ are plotted in Figure 10 vs the viscosity-average molar masses M_v, which were calculated according to eq 12. The parameters of the KMHS equation for polydisperse fractions of linear THV samples in MEK at 35 °C are determined by a linear regression as:

$$[\eta]_{THV}(\text{MEK},35°\text{C}) = 5.1 \times 10^{-3} M_v^{0.739} \tag{15}$$

The intrinsic viscosities $[\eta]$ measured for the LCB-THV are listed in Table 3 and found to be lower than those of linear THV with the same molar mass and the mean contraction factor or so-called branching index g_η is calculated as the ratio of the intrinsic viscosity of the branched sample $[\eta]_{br}$ to that of a linear sample $[\eta]_{lin}$:

$$g_\eta = \frac{[\eta]_{br}}{[\eta]_{lin}} \tag{16}$$

The highest possible number of long-chain branches LCB_{max} can be estimated from the polymerization recipe. Herein, the amount of branching agent utilized as well as the average monomer molar mass of $M_0 = 87.5$ g/mol are taken into account. The values calculated for LCB_{max} are provided in Table 2. The function of g_η is plotted in Figure 11 as a function of LCB_{max}. The contraction factors g_η are found to be smaller than 1 for all LCB-THV, and in particular, they decrease with higher numbers of LCB_{max}. This behavior can be explained by an increasing degree of long-chain branching originating from a higher number of incorporated branch points during the course of polymerization.

The contraction factor g_η can also be determined simultaneously together with g_s for monodisperse fractions of the long-chain branched samples by using the universal calibration for SEC-MALLS. This procedure was previously described in the literature, e.g., by Tackx and Tacx.[29] The intrinsic viscosity of the branched THV samples $[\eta]_{br}$ is calculated from the intrinsic viscosity and molar mass M of the polystyrene standards (eqs 10 and 11) and compared to $[\eta]_{lin}$ as determined from eq 13. The values of g_η are plotted in Figure 12 as a function of M_{LS}. For low molar masses they are equal to 1 and decrease with increasing molar mass. The higher the average molar mass of the samples the higher is the onset molar mass of the decrease in g_η. A similar shape of the molar mass dependence is observed for all long-chain branched samples. That means, that the topography of the samples is comparable. However, the values of $g_\eta(M_v)$ determined from *off-line* viscometry are lower compared to values from *on-line* measurements by SEC-MALLS where $g_\eta(M_v) \approx 1$. The reason for this discrepancy is yet unknown, but one has to take into account that different solvents and temperatures were used.

Branching Parameter ϵ. The intrinsic viscosity and the radius of gyration are two different quantities, which both describe the hydrodynamic volumes of molecules. The contraction factors g_η and g_s at the same molar mass M are related by the exponent ϵ if g_s, $g_\eta < 1$:

$$g_\eta = g_s^{\epsilon} \tag{17}$$

Table 3. Molecular Characteristics of the Long-chain Branched THV Samples as Determined from Viscometry

	LCB-THV 1	LCB-THV 2	LCB-THV 3	LCB-THV 4	LCB-THV 5	LCB-THV 6
M_v [kg/mol]	501.4	625.2	697.9	935.1	491.1	1200.2
$LCB_{max}/10^4C$[a]	0.31	0.91	2.64	6.55	2.7	2.7
$[\eta]_{br}$[b] [mL/g]	78	74.5	74.5	84	102	56
g_η[b]	0.946	0.768	0.708	0.643	0.649	0.69

[a] Calculated from the amount of branching agent added. [b] Determined in MEK at 35 °C using a Cannon−Fenske viscometer.

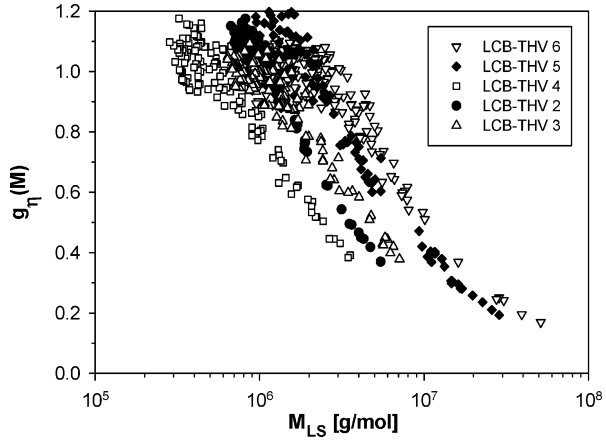

Figure 12. Contraction factor g_η as a function of molar mass M_{LS} for different LCB-THV.

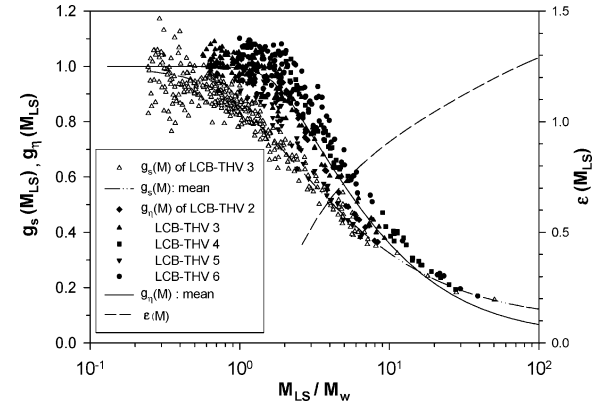

Figure 13. Master curve of $g_\eta(M_{LS})$ and $g_s(M_{LS})$ as well as $\epsilon(M_{LS})$ as a function of the reduced molar mass M_{LS}/M_w.

The Flory−Fox equation predicts that ϵ is equal to $^3/_2$. Later Berry and Orofino[30] derived the same value for comb-shaped molecules having branches, which are relatively small compared to the backbone. Burchard[31] reports ϵ values of $^3/_2$ for comb branched molecules. In the case of nondrained star branched molecules, a value of $\epsilon = {}^1/_2$ was predicted by Zimm and Kilb[32] as the limiting value for an increasing number of long-chain branches. Values in the theoretical range of $0.5 < \epsilon < 1.5$ have been found experimentally for various polymers and reviewed by Shiga,[33] for example.

Since the two contraction factors g_s and g_η are known as a function of molar mass for the LCB-THV samples, the branching parameter ϵ can be calculated. For the long-chain branched THV samples a reduced plot was used, which corrects for the different molar masses. By using the ratio M_{LS} over M_w a master curve for g_η is obtained for the long-chain branched samples (cf. Figure 13). A reasonably good superposition of the data of $g_\eta(M_{LS}/M_w)$ is observed. Thus, the molar mass range has been extended. Furthermore, the master curve of g_η indicates that a similar branching structure can be assumed for these materials. This finding allows the comparison with the function g_s of LCB-THV3. The contraction factors $g_s(M_{LS}/M_w)$ and $g_\eta(M_{LS}/M_w)$ are equal to 1 for small reduced molar masses but show a decrease at higher ones, indicating that long-chain branches are only present in the high molar region ($M_{LS} > M_w$).

The branching parameter $\epsilon(M_{LS}/M_w)$ is calculated from fits of the experimental data of $g_s(M_{LS}/M_w)$ and $g_\eta(M_{LS}/M_w)$ by arbitrarily chosen sigmoid four parameter distribution functions and also shown in Figure 13. It increases with molar mass from about 0.5 to 1.3. This finding is in agreement with results found for LDPE by Beer et al.[34] The change in $\epsilon(M)$ with increasing molar mass corresponds to a change in the branching topography from starlike to comblike.[35] This is quite reasonable also from the branching and polymerization process, respectively.

Conclusions

The TFE/HFP/VDF terpolymer (THV) samples investigated in this study are soluble in common organic solvents. Thus, standard characterization techniques can be applied to these semi-fluorinated copolymers for the determination of the molar mass distribution and the molecular structure in dilute solution. Furthermore, the molecular mass and the chain topography of these fluorinated copolymers can well be controlled by the polymerization recipe. For these reasons, the THV samples analyzed herein are well suited as a model system to study branching effects in general.

Copolymers of different molar masses but narrow molar mass distributions were synthesized. Since undesired side reactions were suppressed during the polymerization process, samples with a straight linear chain topography were attained. Molar mass distributions have been measured with the combination of SEC and MALLS to obtain absolute molar mass values and to determine the KMHS parameters for the universal calibration method. The obtained scaling law parameters are typical of linear chains in good solvents. The experimental data of the THV samples show a very good agreement with the Schulz−Zimm distribution function. The degree of coupling, related to the type of preferred termination reaction, reasonably lies in the range between 1 (recombination) and 2 (disproportionation).

Well-defined trifunctional long-chain branched topographies were efficiently introduced in another set of samples. In SEC-MALLS measurements, the presence of long-chain branches could be revealed by a significantly depressed radius of gyration for polymer fractions in the molar mass region above 10^6 g/mol. But due to experimental uncertainties, the SEC-MALLS method is not sensitive enough to detect long-chain branching for fractions of lower molecular weight as well. The polymer architecture also becomes evident from batch measurements of the intrinsic viscosity recorded on the nonfractionated solutions of the polydisperse samples. Confirming the expectations from the reaction kinetics of the polymerization process, all samples show contraction factors g_η significantly below 1, and furthermore, g_η monotonically decreases with the amount of branching agent utilized.

The contraction factor g_η from SEC-MALLS measurements shows that the branching topography is similar for all samples under investigation as proven by the same molar mass dependence in a reduced molar mass plot. The branching parameter ϵ calculated from $g_\eta(M)$ and $g_s(M)$ increases with growing molar

mass. The calculated values of ϵ suggest a change from a starlike topography at low molar masses to a comblike one at higher molar masses.

Acknowledgment. The authors thank the Bayerische Forschungsstiftung for financial support of this project (File Number 608/04). The authors also gratefully acknowledge the technical support as well as valuable comments from Drs. C. Johann, D. Roessner, and J. Wellensiek of Wyatt Technology Europe (WTE).

References and Notes

(1) Scheirs, J. In *Modern Fluoropolymers*; Scheirs, J., Ed.; Wiley Science New York, 1997.
(2) Ameduri, B.; Boutevin, B.; Kostov, G. *Prog. Polym. Sci.* **2001**, *26*, 105−187.
(3) Logothetis, A. *Prog. Polym. Sci.* **1989**, *14*, 251−296.
(4) Hougham, G.; Johns, K.; Cassidy, P. E.; Davidson, T. *Fluoropolymers: Synthesis and Properties*; Plenum Press: New York, 1999.
(5) Bekiarian, P. G.; Gilmore, P. T. United States Patent 4,612,357, 1986.
(6) Maccone, P.; Apostolo, M.; Ajroldi, G. *Macromolecules* **2000**, *33*, 1656−1663.
(7) Long, V. C.; Berry, G. C.; Hobbs, L. M. *Polymer* **1964**, *5*, 517−524.
(8) Münstedt, H.; Laun, H. M. *Rheol. Acta* **1981**, *20*, 211−221.
(9) Gahleitner, M. *Prog. Polym. Sci.* **2001**, *36*, 895−944.
(10) Vega, J.; Aguilar, M.; Peón, J.; Pastor, D.; Martínez-Salazar, J. *e-Polym.* **2002**, No. 46, 1−35.
(11) Kaspar, H.; Hintzer, K.; Weilandt, K. D.; Krichel, J.; Peters, Internat. Patent Publication WO 02/88203, 2002.
(12) Benoit, D. W.; Grubisic, Z.; Rempp, P. *J. Polym. Sci., Part B:* **1967**, *5*, 753−759.
(13) Sun, T.; Chance, R. R.; Graessley, W. W.; Lohse, D. J. *Macromolecules* **2004**, *37*, 4304−4312.
(14) Shortt, D. W. *J. Liquid Chrom.* **1993**, *16*, 3371−3391.
(15) Zimm, B. *J. Chem. Phys.* **1948**, *16*, 1093−1099.
(16) Huglin, M. B. In *Light Scattering from Polymer Solutions*; Huglin, M. B., Ed.; Academic Press: London, 1972.
(17) Zimm, B. H.; Dandliker, W. B. *J. Phys. Chem.* **1954**, *58*, 644−648.
(18) Hadjichristidis, N.; Fetters, L. J. *J. Polym. Sci.* **1982**, *20*, 2163.
(19) Brandrup, J.; Immergut, E. H.; Grulke, E. A. *Polymer Handbook*, 4th ed.; Wiley: New York, 1999.
(20) Jones, N.; Chen, Y.-J.; Mays, J. W. *J. Appl. Polym. Sci.* **1996**, *61*, 865.
(21) Jeng, L.; Balke, S. T.; Mourey, T. H.; Wheeler, L.; Romeo, P. *J. Appl. Polym. Sci.* **1993**, *48*, 1359.
(22) Elias, H. G. In *Makromoleküle−Band I−II*, 6. Aufl.; Wiley-VCH: Weinheim, Germany, 2001.
(23) Mori, H.; Seng, D. C.; Lechner, H.; Zhang, M.; Müller, A. H. E. *Macromolecules* **2002**, *35*, 9270−9281.
(24) Flory, P. J.; Fox, T. G *J. Polym. Sci.* **1950**, *5*, 745.
(25) Flory, P. J. *Principles of Polymer Chemistry*, 16th ed.; Cornell University Press: Ithaca, NY, 1953.
(26) Jackson, C.; Chen, Y.; Mays, J. W. *J. Appl. Polym. Sci.* **1996**, *59*, 179−188.
(27) Gabriel, C.; Münstedt, H. *Rheol. Acta* **2002**, *41*, 232−244.
(28) Zimm, B. H.; Stockmayer, W. H. *J. Chem. Phys.* **1949**, *17*, 1301−1314.
(29) Tackx, P.; Tacx, J. C. J. F. *Polymer* **1998**, *39*, 3109−3113.
(30) Berry, G. C.; Orofino, T. A. *J. Chem. Phys.* **1964**, *40*, 1614.
(31) Burchard, W. *Adv. Polym. Sci.* **1999**, *143*, 156.
(32) Zimm, B.; Kilb, R. W. *J. Polym. Sci.* **1959**, *37*, 19−42.
(33) Shiga, S. *Polym. Plast. Techn. Eng.* **1989**, *28*, 17−41.
(34) Beer, F.; Capaccio, G.; Rose, L. J. *J. Appl. Polym. Sci.* **2001**, *80*, 2815−2822.
(35) Berry, G. C. *J. Polym. Sci., Part B: Polym. Phys.* **1988**, *26*, 1137−1142.

MA051391A